

Analysis of Seismic Time-Depth Conversion Using Geostatistically- Derived Average Velocities over “Labod” Field, Niger Delta, Nigeria

Olabode O. P. and Enikanselu P. A.

Department of Applied Geophysics, Federal University of Technology, P.M.B. 704, Akure, Ondo State, Nigeria

Email: paenikan@yahoo.com

Abstract: *Geostatistical techniques were used for seismic time-depth conversion over “Labod” field offshore Western Niger Delta Basin with the aid of surface seismic and borehole data. Gamma ray and resistivity logs in four exploratory wells were utilized to delineate formation lithologies (facies) and formation fluid content. The target horizon B (top of sand 2) was selected for seismic structural mapping. Two major faults (F_1 , F_2) and three minor faults (F_3 , F_4 and F_5) were identified and interpreted on the seismic sections. Average velocities were first calculated from sonic logs. Geostatistical techniques - Kriging with External Drift (KED) and Simple Kriging - were employed to generate average velocity models used to convert the target B seismic time surface to depth in and away from well locations and depth maps were generated. The results of maximum percentage deviation computed among field-observed and computed depths were lower than 5% suggesting that the average velocity values estimated away from wells were reliable and applicable especially in areas where there is scarcity of well information. The Kriging with External Drift (KED) technique is particularly recommended because of the higher accuracy and denser data coverage. Finally, the method is cost effective because only few wells are required to achieve the expected results.*

Keywords: Geostatistical; Facies; Horizons; Faults; Average velocity; Variogram; Kriging

INTRODUCTION

The primary geophysical seismic data is often recorded in time. However, meaningful interpretation needs be displayed in depth. The primary objective of geophysical seismic interpretation is to prepare contour seismic maps showing the two way time to a reflector as picked on the seismic sections. This time (isochron) map must be converted to depth (isodepth) map through the seismic time-depth conversion process. The depth conversion process is usually carried out using formation average velocity information derived from well data. Geostatistical techniques, Iyiola *et al.*, (2000), have been used to improve seismic time-depth conversion, which resulted in a significant increase in reservoir volume above the oil water contact over the result obtained from common techniques.

Geostatistics is the application of statistical estimation techniques to spatially correlate random variables for geological and geophysical applications, Sheriff (1999). Generally, as the distance between two data points increases, the similarity between the two measurements decreases, Chambers *et al.*, (2000). The application of geostatistics in estimating accurate velocities for proper depth conversion of the reservoir is necessary to accurately estimate reserves and optimize the placement of development wells.

However, velocity information derived from the existing wells is spatially too sparse to adequately delineate the lateral velocity variations, Hwang and McCorkindale (1994). Hence, seismic time to depth conversion is usually problematic due to the larger number of variables that influence the velocities. These variables - porosity, compaction, under compaction, e.t.c.- make it difficult to derive the correct velocity information and corresponding depth structure. Since a unique velocity solution is presumed inadequate, a probabilistic model of the velocity may be realistic. To build such a model, we need to make sure that it incorporates geologically feasible lateral and vertical velocity variations and all available well information.

This work analyses two other schemes – statistical regression of seismic time and average velocity and the Kriging technique and compares them with the conventional borehole (sonic) model of average velocity estimation. These methods have the advantage of largely improving spatial data density and extrapolating velocities between and away from borehole locations.

Location & Geology of the Study Area

The “Labod” field is located offshore western Niger Delta. It covers an area of about 55,388,125 ft² (16,754,908 m²), Figure 1. The geology of the Tertiary section of the Niger Delta is divided into three Formations, representing prograding depositional facies distinguished mostly on the basis of sand-shale ratio (Short and Stable, 1967; Doust and Omatsola, 1990; Kulke, 1995). They are namely Benin Formation, the Paralic Agbada Formation and Prodelta Marine Akata Formation. They range in age from Paleocene to Recent. The Benin Formation is a continental latest Eocene to Recent deposit of alluvial and upper coastal plain sands. It consists predominantly of freshwater baring massive continental sands and gavels deposited in an upper deltaic plain environment. The Agbada Formation consists of paralic siliciclastics, which underlies the Benin Formation. It consists of fluviomarine sands, siltstones and shales. The sandy parts constitute the main hydrocarbon reservoirs. The grain size of these reservoir ranges from very coarse to fine. The Akata Formation is the basal unit of the Tertiary Niger Delta complex. It is of marine origin and composed of thick shale sequences (potential source rock), turbidities sand (potential reservoirs in deep water and minor amount of clay and silt. Beginning in the Paleocene and through the Recent, the Akata Formation formed during low stands, when terrestrial organic matter and clays were transported to deep-sea water areas characterized by low energy conditions and oxygen deficiency (Stacher, 1995). It is the major source rock in the Niger Delta.

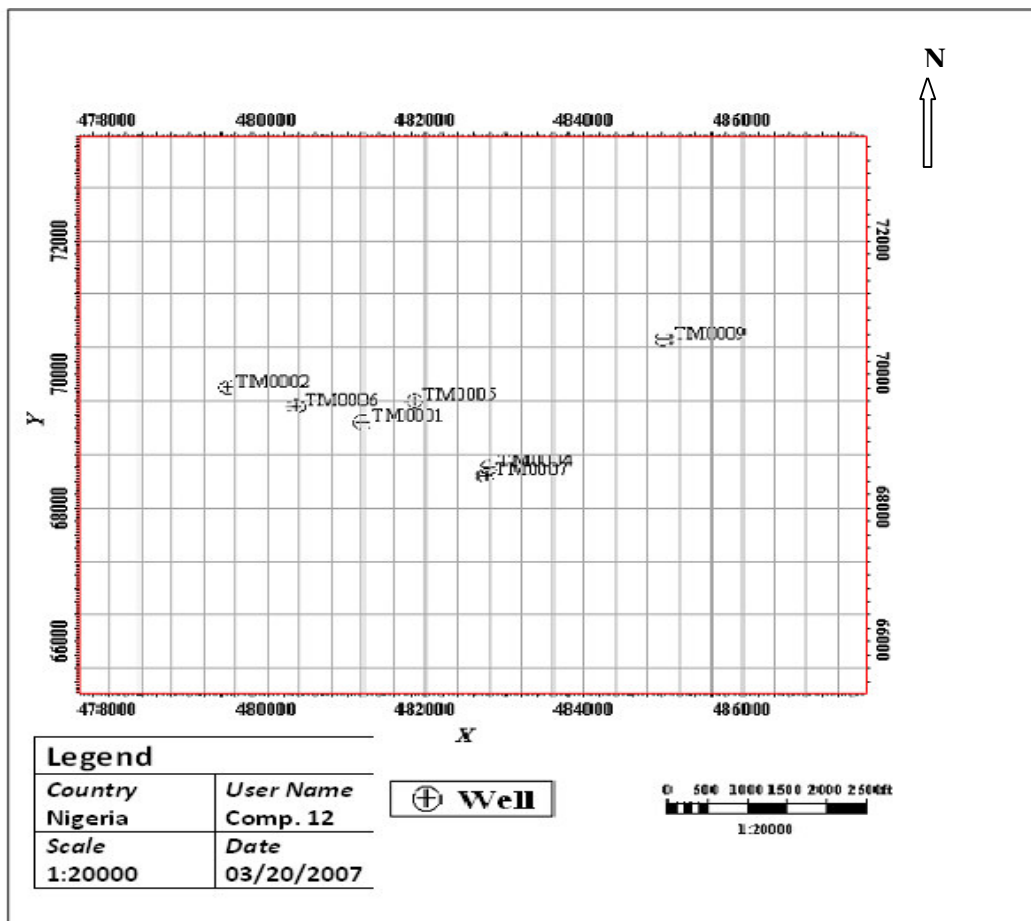


Figure 1. Basemap of “Labod” Field Showing Well Locations and Seismic Lines.

MATERIALS AND METHODS

The main data comprised 3-D seismic sections and borehole data (sonic log, density, gamma ray log, resistivity logs and checkshots). Gamma ray and resistivity logs were used to delineate lithofacies in four – 1, 2, 4 and 6 -

of the seven wells. The target 'B' horizon was identified on both the well logs and seismic sections. Faults were also identified and interpreted as fault planes.

The B-time surface was converted to depth using average velocities derived from sonic logs from six wells. Also, average velocities were calculated from check shots data from six wells and a spherical model variogram was built for these velocities in both major and minor directions and kriging with external drift was used to predict average velocities away from the wells by linear regression. The resultant average velocity map was again used to convert the B surface to depth.

Finally, the kriging formulation was employed to estimate average velocity values away from well locations to boost spatial data density. The resultant velocity distribution was then used to convert the surface to depth. The percentage variation of the converted depths depth among the three techniques was analyzed to determine the level of accuracy and reliability of the geotechnical techniques.

PRESENTATION AND DISCUSSION OF RESULTS

For the purpose of this work, the sources of the data were the surface seismic and subsurface borehole data. Sixty-two seismic reflection lines (40 inlines and 22 crosslines) and composite well logs from six wells, spaced over an area of about 55,388,125 sq. ft. (16,754,908 m²) were used for the study. The wireline logs comprised gamma ray, resistivity, sonic, density logs and check shots data.

Seismic structural interpretation was carried out on the seismic sections to produce seismic time maps and fault planes. Also, geostatistical techniques were used to generate average velocity maps that were used for time-depth conversion. These techniques were variogram analysis, Regression and Kriging. The results were presented as maps and tables. The output of the model was compared with the available subsurface borehole field data. Figure 2 shows the top of the mapped sand in well TM0006 corresponding to the target B horizon, Figure 3. The available check shot data from the wells facilitated the change from the measured depth (5484ft or 1672 m, Figure 2) to two way seismic travel-time 1.906 seconds, Figure 3. The deep resistivity log assisted in revealing the reservoir fluid content – hydrocarbon or water.

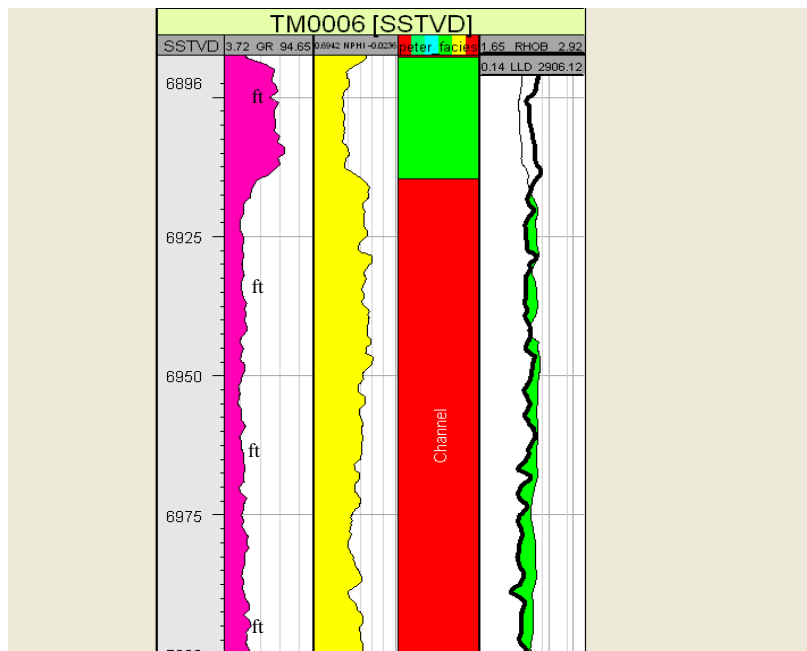


Figure 2. Top of Sand-2 as revealed in Well TM0006

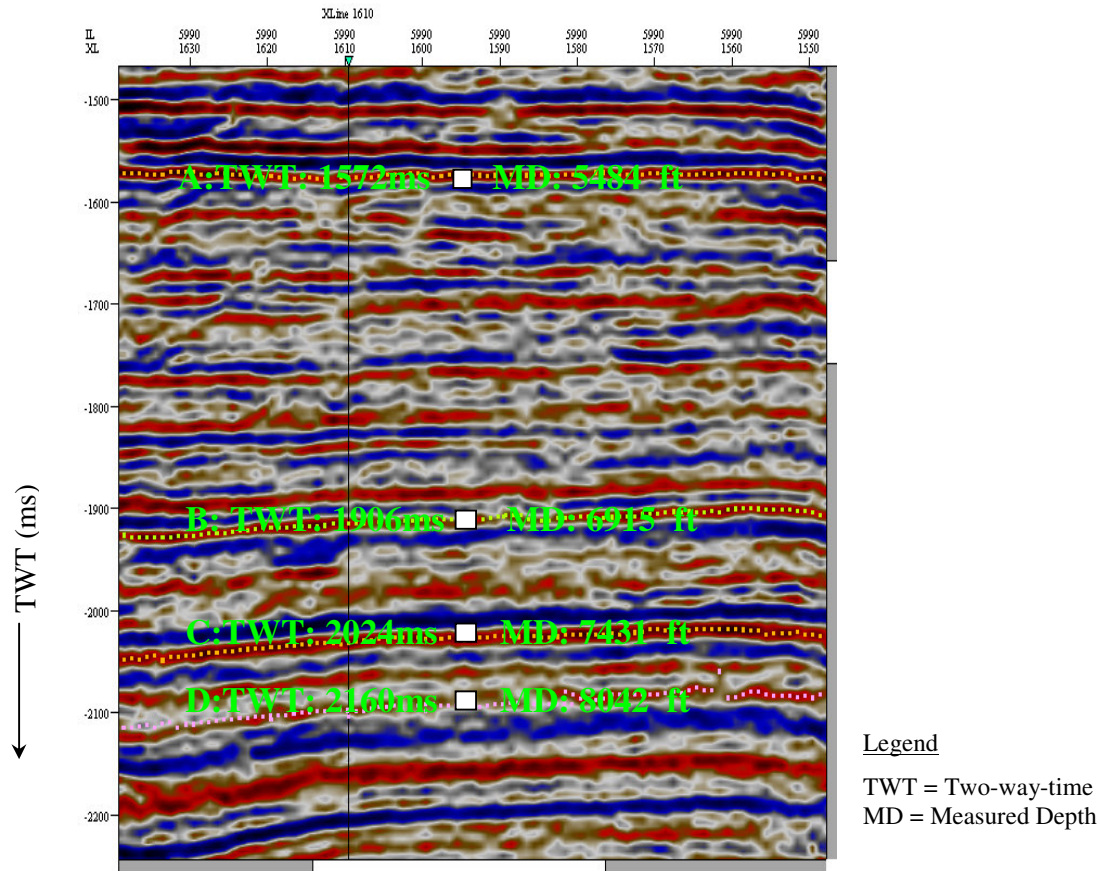


Figure 3. The Four mapped Seismic Time Horizons and their Depth Coordinates on Inline 5990

Figure 4 is the seismic structural time map of the target B-surface (Top of sand 2). Five faults, F1, F2, F3, F4, and F5, were delineated on the seismic sections. F1 and F2 were the growth faults (major structure) that bound the field. F1 was located at the north while F2 was located at the southern part of the field. They both strike eastwest and dip south directions. Faults F3, F4, and F5 were minor faults. F3 was located between the two growth faults striking northsouth and dipping west. F4 and F5 were located at the extreme northeast and both strike in northwest-southeast and dip in southwest directions. The average velocities derived from sonic logs were used to convert the target seismic B-surface to depth, Figure 5.

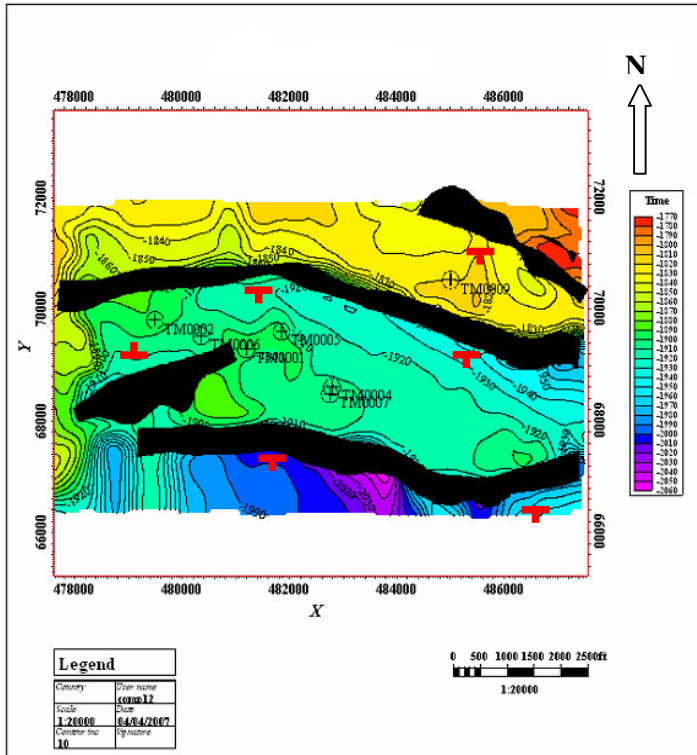


Figure 4. Structural Time Map of the target B surface.

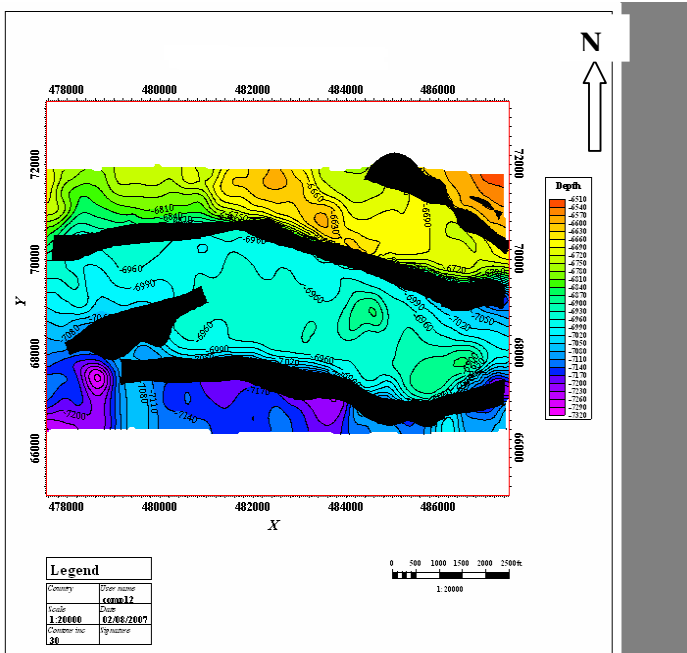


Figure 5. Structural Depth Map of B surface Derived from Sonic Velocity.

The converted depths range from 6680 ft (2004m) in well 9 to 6997 ft (2099m) in Well 6. This revealed the dipping nature of the surface. The difference of 317ft (95m) observed on the surface was suspectedly attributed

to the high rate of variation of basin subsidence compared to deposition (Doust and Omatsola, 1990; Turtle *et al.*, 1999).

The difference of 40ft (12m) depth between Wells 6 and 2 was equally suspected to be due to continuous downward dragging of sediments in the active downthrown side of fault F3. Figure 6 shows the anisotropic variograms of the average velocities derived from check shots data in six Wells.

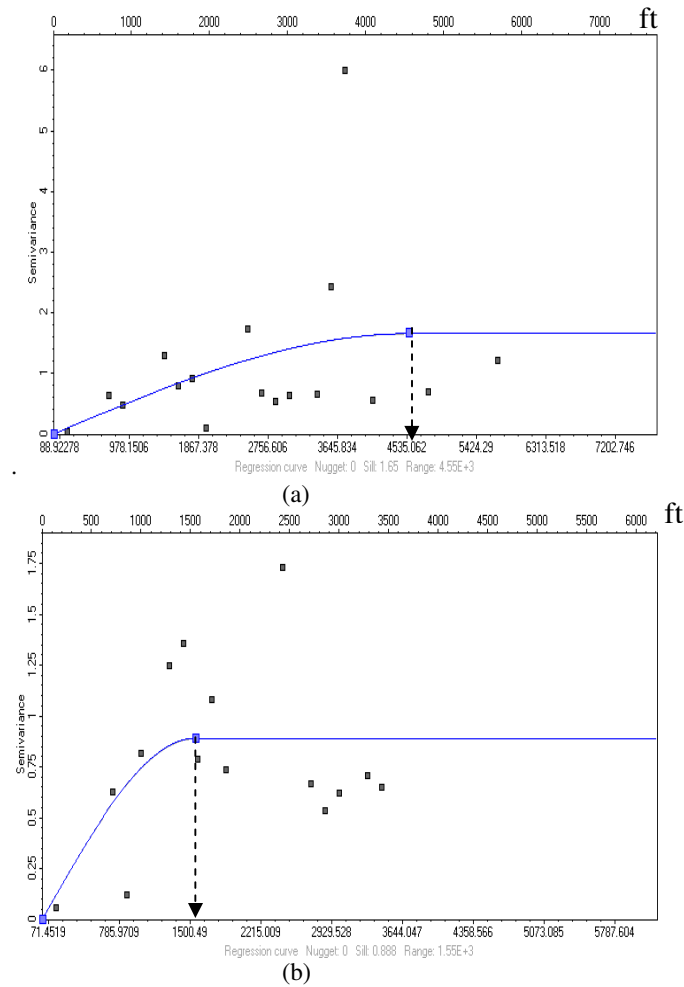


Figure 6: Observed Variogram in (a) Major range Direction and (b) Minor Direction

A spherical variogram model was used with a range of 4551ft and 1551ft in major and minor directions respectively and zero nugget effect. Figure 7, the resultant average velocity map, was derived using Kriging with External Drift (KED). The computed high positive correlation between two-way time and average velocities in the wells, with correlation coefficient of 0.992, had highly facilitated the prediction of velocities away from the wells. The average velocity values at the wells were similar because the variogram model has zero nugget effect. The obtained average velocity values are a linear function of time, within the variogram range of 4551ft and 1551ft in both major and minor directions respectively, Dubrule (2003). The average velocity map displayed a general trend striking eastwest and dipping northsouth. The trend of the average velocity follows the major geologic structure (faults) expected in the study area (Hwang and Mc-Corkindale, 1994).

Figure 8 shows the depth map of the B- surface obtained from Figure 7. The depth map is similar in structure to the sonic-derived depth map, Figure 5. It could be observed that the contour value 6930 ft between faults F1 and F2 in Figure 8 coincides with contour value 6960ft in Figure 5, thus revealing a 30ft (9m) difference in depth between the two maps.

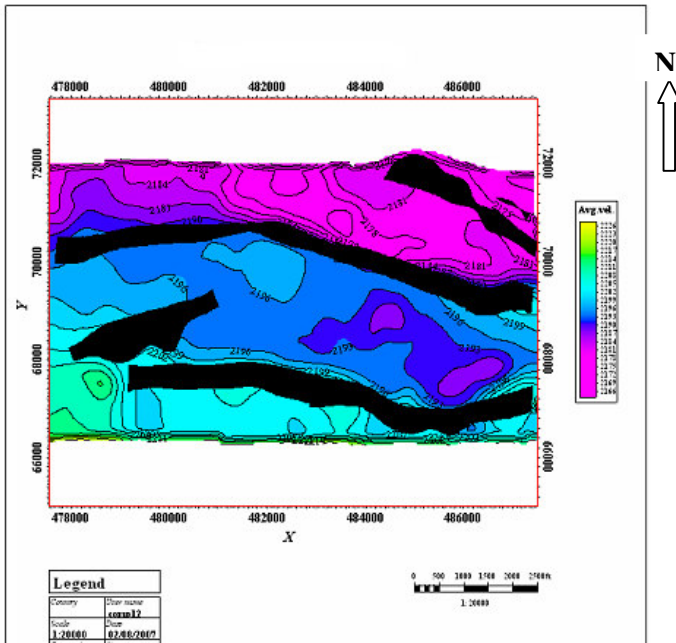


Figure 7. Average Velocity Map derived from Kriging with External Drift (KED).

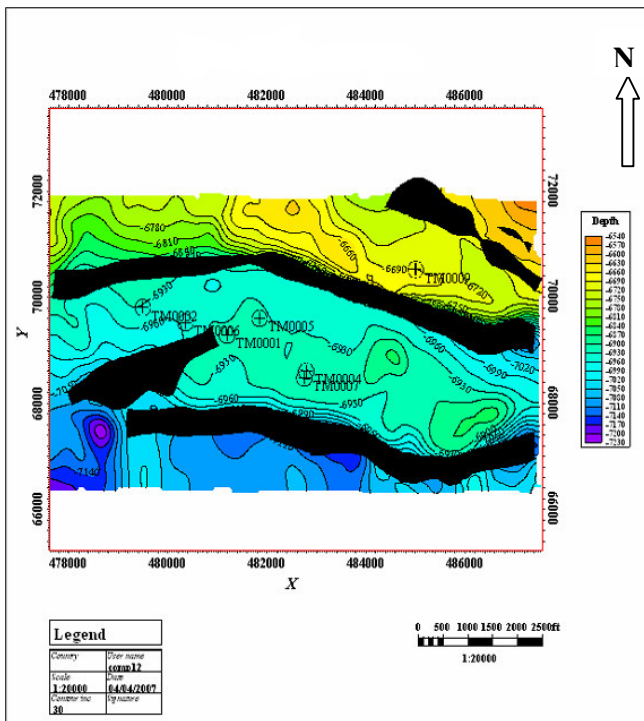


Figure 8. The depth map of the B- surface derived from Kriging with External Drift (KED).

Figure 9 shows the average velocity map of the B- surface using simple Kriging technique with grid node interval of 100ft. It was generated from the computed velocities at the nodal points of the gridded B- surface in the area.

Table 1 showed the converted depths and the percentage deviations between them using average velocities derived from sonic logs (Z_S) when compared with those obtained using Kriging with External Drift (Z_{KED}) and Kriging (Z_K) respectively. The results show a maximum percentage deviation of 0.91% for Z_{KED} and 4.91% for Z_K (both less than 5%). These suggested that the average velocities estimated away from the well locations using geostatistical techniques were reasonably reliable. It could be observed that the deviations increased as one moves away from the well locations. This is in agreement with geostatistics on spatial distribution of random variables (Wolf *et al.*, 1994). Beyond the variogram range, Figure 6, the predicted values become unreliable. It suggests that at a shorter range, the prediction is more effective than at a larger range away from well locations. Since there are near uniformity in the percentage deviation of Z_{KED} than Z_K around the wells location, the Regression analysis using Kriging with external Drift is a more preferable method than Kriging.

S/N	X-coord.	Y-coord.	Z_S (ft)	Z_{KED} (ft)	Z_K (ft)	% Deviation $\frac{ Z_S - Z_{KED} }{Z_S} \times \frac{100}{1}$	% Deviation $\frac{ Z_S - Z_K }{Z_S} \times \frac{100}{1}$
1	483600	66600	-7200	-7140	-6920	0.83	3.89
2	480400	66800	-7140	-7110	-6970	0.42	2.38
3	482000	67200	-7170	-7110	-6937	0.83	3.25
4	485200	67200	-6990	-6960	-6914	0.43	1.09
5	483600	67800	-6990	-6960	-6917	0.43	1.04
6	480400	68000	-7020	-6990	-6980	0.43	0.57
7	482000	68000	-7020	-6990	-6935	0.43	1.21
8	483600	68000	-6960	-6930	-6919	0.43	0.59
9	482000	68200	-6990	-6960	-6935	0.43	0.79
10	480400	68400	-6960	-6930	-6985	0.43	0.36
11	485200	68400	-6930	-6900	-6923	0.43	0.10
12	486800	68600	-7020	-6990	-6915	0.43	1.50
13	485200	69000	-6960	-6930	-6929	0.43	0.45
14	483600	69200	-6960	-6930	-6950	0.43	0.14
15	482000	69800	-6960	-6930	-6965	0.43	0.07
16	486800	69800	-6750	-6750	-6918	0	2.49
17	485200	70000	-6720	-6750	-6938	0.45	3.24
18	480400	71000	-6840	-6840	-6994	0	2.25
19	485200	71000	-6690	-6720	-6945	0.45	3.81
20	486800	71000	-6600	-6660	-6920	0.91	4.85
21	482000	71200	-6660	-6690	-6987	0.45	4.91
22	483600	71200	-6660	-6690	-6975	0.45	4.73

Table 1. Comparison of Converted Depths at 22 Sampled Locations in the Study Area.

CONCLUSION

In this study, we have attempted to analyse the concept of seismic time to depth conversion using the approach of borehole logs and geostatistical tools. The subsurface reservoir trapping mechanism of the area was revealed to be a fault-assisted anticlinal structure. The average velocity values estimated using geostatistical techniques were reliable for the time-depth conversion because the maximum percentage deviation computed between the observed field data and the estimated geostatistical depths, was less than 5%. The statistical regression analysis of average velocity and seismic two-way time (TWT) revealed the feasibility of generating average velocities from seismic times in areas where well information is sparse. The low percentage deviation between the conventional and geostatistical approaches in time-depth conversion lends credence to the reliability of adopting the latter. The Kriging with External Drift (KED) technique is particularly recommended because of the higher accuracy and the potential of generating denser data coverage. This technique is useful especially in areas where there is scarcity of well information. Lastly, the method is cost effective because only few wells are required to achieve the expected results.

We strongly recommend that more detailed analysis be carried out on this subject using other geostatistical techniques such as Sequential Gaussian Simulation (SGS) method with seismic attributes - stacking velocities, acoustic impedance etc - integrated with well data.

ACKNOWLEDGEMENT

The authors are grateful to the Department of Petroleum Resources for granting our request for data with which the research was accomplished. Also, we appreciate the benevolence of the Department of Applied Geophysics, Federal University of Technology, Akure, Nigeria, for the use of the Schlumberger-donated Petrel workstation.

REFERENCES

- Chambers R. L., Yarus, J. M. & Hird, K. B. (2000). Petroleum Geostatistics for Non-Geostatistics, The Leading Edge, Pg. 474-479.
- Doust, H., and Omatsola, E. (1990). Niger Delta, in, Edwards, J. D., and Santogrossi, P. A., Eds., Divergent/Passive Margin Basins, AAPG Memoir 48: Tulsa, American Association of Petroleum Geologists, Pg. 239-248.
- Dubrule, O. (2003). Geostatistics for Seismic Data Integration in Earth Models, Sponsored by Society of Exploration Geophysicists and European Association of Geoscientist and Engineers Distinguish Instructor Series, No. 6.
- Hwang, L. and McCorkindale, D. (1994). Troll Field Depth Conversion Using Geostatistically Derived Average Velocities. The Leading Edge, Vol. 13, Pg. 262-269.
- Iyiola, O.T., Bee, M. F. and Jekins, S. (2000). Using Geostatistical Techniques to improve Depth conversion in Robertkiri Field, Nigerian Association of Petroleum Explorationists Bulletin, vol, 15, pp. 16 – 28.
- Kulke, H., (1995). Nigeria, In, Kulke, H., Ed., Regional Petroleum Geology of the World. Part II: Africa; America; Australia And Antarctica: Berlin, Gebrüder Borntraeger, Pg. 143-172.
- Sheriff, F. R. (1999). Encyclopedia Dictionary of Exploration Geophysics, Third Edition, Society of Exploration Geophysicists.
- Short, K. C., and Stauble, A. J. (1965). Outline of Geology of Niger Delta: American Association of Petroleum Geologists Bulletin Vol. 51, Pg. 761-779.
- Stacher, P. (1995). Present Understanding of the Niger Delta Hydrocarbon Habitat, In, Oti, M. N., and Postman Eds., Geology of Deltas: Rotterdam, A. A., Balkema, Pg. 257-267.
- Turtle, M. L.W., Charpentier, R. R., and Brownfield, M. E. (1999). The Niger Delta Petroleum System: Niger Delta province, Nigeria, Cameroon and Equatorial Guinea, Africa, USGS.
- Wolf, D. J., Withers, K. D., and Burnaman, M. D. (1994). Integration of Well and Seismic Data Using Geostatistics: AAPG Computer Applications in Geology, No 3 pp. 177-196.